Heliyon 10 (2024) e37813

Contents lists available at ScienceDirect

Heliyon

journal homepage: www.cell.com/heliyon

Research article

Deactivation and regeneration dynamics in hierarchical zeolites: Coke characterization and impact on catalytic cracking of vacuum gas oil

Jayson Fals [a,*], Maria L. Ospina-Castro [b], Andrea Ramos-Hernández [b], Leonardo Pacheco-Londoño [c,**], Sonia Bocanegra [d]

[a] Grupo de Investigación en Oxi/Hidrotratamiento Catalítico y Nuevos Materiales, Programa de Química-Ciencias Básicas, Universidad del Atlántico, Barranquilla, Colombia
[b] Grupo de Investigación Química Supramolecular Aplicada, Ciencias Básicas, Universidad del Atlántico, Puerto Colombia, Colombia
[c] Centro de Investigaciones en Ciencias de la Vida, Facultad de Ciencias Básicas y Biomédicas, Universidad Simón Bolívar, 080002, Barranquilla, Atlántico, Colombia
[d] Instituto de Investigaciones en Catálisis y Petroquímica "Ing.José M. Parera" (INCAPE)- Universidad. Nacional del Litoral, CONICET, RN 168, Km 0 Paraje El Pozo, Santa Fe, Argentina

ARTICLE INFO

Keywords:
Catalytic cracking
Hierarchical zeolites
Coke
Catalyst deactivation
Vacuum gas oil

ABSTRACT

This study investigated the deactivation and regeneration of hierarchical zeolites in vacuum gas oil conversion, aiming to reach the equilibrium state seen in fluidized bed catalytic cracking (FCC). The research utilized various characterization techniques to analyze the properties of zeolites before and after coking and regeneration. Zeolite Y-0.20-S was found to have the highest gasoline selectivity and quality, mirroring industrial yields, and displayed notable stability across deactivation/regeneration cycles. Higher mesopore concentration in zeolites led to increased coke selectivity and better resistance to deactivation. The study observed a dominance of aromatic coke with a higher degree of condensation in these zeolites. Despite coke deposition affecting acid and textural properties, the regeneration process effectively restored these characteristics, proving its efficiency. The zeolites with greater mesoporosity retained their fundamental properties responsible for activity and selectivity, highlighting the importance of selecting materials that provide high conversions and maintain stability and product selectivity over multiple cycles. The Y-0.20-S zeolite, in particular, was identified as a promising candidate for commercial catalyst development for gasoline production, contributing to the FCC process's energy efficiency.

1. Introduction

For decades and continuing into the present, the fluidized bed catalytic cracking (FCC) unit remains a pivotal component in refineries, effectively converting the bottom of the barrel into more valuable outputs like liquefied petroleum gas and high quality

* Corresponding author.
** Corresponding author.
E-mail addresses: jaysonfals@mail.uniatlantico.edu.co (J. Fals), mariaospina@mail.uniatlantico.edu.co (M.L. Ospina-Castro), andrearamos@mail.uniatlantico.edu.co (A. Ramos-Hernández), leonardo.pacheco@unisimon.edu.co (L. Pacheco-Londoño), sbocane@fiq.unl.edu.ar (S. Bocanegra).

https://doi.org/10.1016/j.heliyon.2024.e37813
Received 18 March 2024; Received in revised form 8 September 2024; Accepted 10 September 2024
Available online 11 September 2024

gasoline [1–3]. The usual feedstock for this process is vacuum gas oil (VGO), composed of hydrocarbons in the C_{20}-C_{50} range with an average boiling temperature of approximately 450 °C. The characteristics of the crude oil from which VGO is derived affect its quality, primarily influenced by its density and hydrocarbon family distribution [4–6]. In a conventional FCC process, a zeolitic catalyst back and forth between the cracking reactor and the regenerator [7]. During cracking, the catalyst is mixed with the feed at a temperature of 550 °C, producing a vapor stream composed of several groups of hydrocarbons with different boiling points, while carbonaceous residue accumulates on the material surface. Since the process is cyclical (deactivation/regeneration), the coked catalyst is then sent to a regeneration unit where air and/or steam at high temperatures is used to burn off the coke deposits. Among all the process factors, the temperature at which combustion occurs in the regenerator and the coke content are decisive since the amount of coke can favor the energy balance of the process [8,9].

Commercial FCC catalysts can have different compositions, influencing the catalytic process differently. These are made using zeolite particles dispersed in an amorphous silica-alumina matrix, with zeolite Y being the most widely used. The average particle size of the catalysts is about 70 μm, with the zeolite crystals measuring less than 1 μm [10,11]. The employment of zeolites as the main component of the catalysts presents a significant advantage, since most of their active sites reside within the micropores, and the carbocation generated by adding protons to the reactants is stabilized due to the structure's negative charge. Furthermore, zeolites possess shape selectivity and are known for having strong Brønsted and Lewis acid sites, which favor cracking reactions [12]. In the process, the reagent molecules must diffuse through the porous system to reach the active sites in the microporous structure of the zeolite, adsorb, and react. Thus, acidic and textural properties control the performance of these catalysts [13,14].

The nature of the pore system of zeolite Y causes the reactants to have severe diffusion problems, conditioning the access of bulky molecules larger than the size of the micropores in zeolite Y (7.4 Å) to internal active sites and bulky products, hindering their diffusion to the outside. An alternative to improve the catalytic efficiency of Y zeolites can be considered by using hierarchical zeolites with a developed pore system that mainly comprises mostly mesopores. Alkaline treatment for desilication of zeolites proved to be the most efficient method for generating mesoporous zeolites. At present, many studies of desilication have been carried out using different zeolites, obtaining materials with high porosity, strong acidity, and effective catalytic properties. The Si/Al molar ratio of the zeolite is critical for creating mesoporosity. A low Si/Al ratio hinders selective silicon extraction, whereas a high Si/Al ratio leads to uncontrolled extraction, resulting in excessively large pores. For our study's objectives, the optimal Si/Al ratio range for achieving controlled desilication is between 25 and 50 [15,16].

An additional problem typical of acidic zeolites in the conversion of heavy molecules at high temperatures arises from rapid deactivation, which means that the catalysts must be resistant to coke deposition on their surface. The multiple chemical reactions that occur in the catalytic cracking of hydrocarbons inevitably lead to the deposition of coke, which has a double impact: covering the active acid sites and blocking the pore. The yield and the nature of the coke (H/C ratio, degree of condensation, and structure) arose from the composition of the raw material, the catalyst properties, and the process conditions. Therefore, they will affect the delicate thermal balance of the refineries, based on the combustion of coke in the regeneration unit to supply the heat consumed by the series of general endothermic reactions in the in the riser [17–19]. All the above highlights the importance of studying the properties of coke accumulated on the surface of zeolites produced from hydrocarbon cracking, to implement suitable regeneration methods that can restore the catalyst's original properties and activity.

Laboratory scale experiments play an important role in properly developing a catalyst. In turn, it is of utmost relevance that the results obtained from laboratory tests can be adequately extrapolated to the commercial unit. Catalytic cracking is conditioned by multiple operational variables involved in the process and the extremely rapid deactivation of the catalyst. This estimation is achieved through modeling, which becomes increasingly complex with the discrepancies in operating conditions between laboratory and industrial scales. For instance, extrapolating data from a fixed bed is more challenging compared to a fluidized bed [20]. In certain applications, it is essential to replicate the impact of deactivation/regeneration cycles on catalyst deactivation. To this end, specialized laboratory protocols and configurations have been established for this purpose. Several laboratory units have been developed to simulate the FCC unit reactor, one of the most prominent, together with the riser reactor, is the fixed bed unit (Micro Activity Test, MAT). Fixed bed units, whose most representative methodology has been standardized in the ASTM D-3907 technique, have been utilized for over four decades as the most frequent laboratory test for catalytic cracking. The main advantage of MAT is its extreme simplicity of operation. Even without shaping the microspheres, only a few grams of catalyst are needed, and tests can be performed in automated units with minimal operating costs [21–23].

Some investigations have studied the deposition of coke in the cracking intending to reveal its formation mechanism and its impact on the deactivation of the catalyst [24–26]. However, there needs to be more research on the evolution of catalyst properties during deactivation/regeneration cycles. Combustion regeneration is a process that involves several reactions coupled with heat and mass transfer on multiple scales that affect catalyst durability and lifetime. In this work, we studied the evolution of the properties of hierarchical zeolites during and after several deactivation/regeneration cycles in the catalytic cracking of a Colombian VGO using a fixed bed reactor (MAT). In addition, the characteristics of the coke deposited on the surface of the zeolites, the effect on its properties (acidic and textural), and the distribution and quality of the products obtained were studied.

2. Experimental section

2.1. Feedstock characterization

A Colombian paraffinic VGO was used as feedstock in the work. The feedstock properties were determined employing the following analytical techniques. The API gravity was measured according to ASTM D287-12b [27]. The Conradson carbon residue (CCR) was

determined using a calcination method based on ASTM D4530-15 [28]. The saturated, aromatic, resin, and asphaltene (SARA) fractions of the VGO were quantified using the method outlined in ASTM D2007-11 standard [29]. The simulated distillation curves were obtained in a Shimadzu GC-2014 gas chromatograph, following the ASTM D2887-23 standard [30]. The elemental composition (content of vanadium, nickel, sodium and iron) was analyzed using inductively coupled plasma optical emission spectroscopy (ICP-OES) with a PerkinElmer model OPTIMA 7300 DV spectrometer.

2.2. Alkaline treatment of Y zeolite

Four Y zeolites with varying levels of intracrystalline mesoporosity were obtained. The starting material was a commercial Y zeolite with Si/Al = 31 ratio. The zeolite CBV 760 in its protonic form was provided by Zeolyst International. Three aqueous solutions of sodium hydroxide with different concentrations were prepared: 0.10, 0.20 and 0.30 mol/L. Five grams of the parent zeolite were dissolved in 200 mL of each aqueous NaOH solution with constant stirring for 10 min at 25 °C and then neutralized with 0.5 mol/L HCl. The samples obtained in the previous step were washed with distilled water and filtered under vacuum conditions. The modified zeolites were subjected to ion exchange with an aqueous solution of 0.50 mol/L NH_4Cl in a rotary evaporator, operating at 25 °C for 8 h with a zeolite/solution ratio of 1 g/10 mL, to eliminate any sodium potentially introduced during the leaching process. Subsequently, it was dried at 110 °C for 12 h and calcined at 550 °C, with the temperature rising at a rate of 10 °C/min from room temperature and held for 2 h. The process yield was determined as the ratio of the mass of zeolite recovered after calcination to the mass of zeolite initially suspended in the alkaline solution. The yields were close to 80 % for each leaching stage. The modified zeolites were the result of the treatment of the original zeolite. The treated and untreated zeolites were steamed during 5 h at 780 °C. The steamed samples were named Y-0.00-S, Y-0.10-S, Y-0.20-S, and Y-0.30-S, respectively, according to the alkali concentration during the treatment. The methodology used for desilication and hydrothermally stabilization was previously described by Fals et al., [25].

2.3. Characterization zeolites

The zeolites were studied before (as fresh zeolites) and after (as coked zeolites) the catalytic cracking experiments. Additionally, their state was assessed after regeneration (as regenerated zeolites). The properties were characterized by X-ray diffraction (XRD), nitrogen physisorption, inductively coupled plasma-optical emission spectrophotometer (ICP-OES), temperature-programmed desorption (TPD) and pyridine temperature-programmed desorption coupled to a Fourier transform infrared spectrometer (Py-FTIR). The textural (surface area, pore volume, and average mesopore diameter) and acidic (nature, strength, and density of acid sites) properties of fresh, coked (after four reaction/regeneration cycles), and regenerated zeolites were evaluated.

The textural properties of fresh, coked, and regenerated zeolites were determined with a 3-FlexTM automatic analyzer from Micromeritics. Initially, the zeolites were degassed at 300 °C for 24 h under vacuum of 10^{-6} mmHg, and adsorption-desorption measurements were performed at T = −196 °C. The specific surface area was measured using the BET (Brunauer-Emmet-Teller) method. Total pore volumes were assessed based on nitrogen adsorption up to a P/Po of approximately 0.98. Mesopore surface areas and micropore volumes were determined using the t-plot method. Mesopore size distributions and average pore diameters were derived from the BJH (Barrett−Joyner−Halenda) model.

The acidic properties (including density of acid sites, strength and nature) of fresh, coked, and regenerated zeolites were assessed using Fourier transform infrared (FTIR) spectroscopy and TPD with pyridine as the probe molecule. The FTIR spectra were collected at a resolution of 4 cm^{-1} and 256 scans using a Nicolet FTIR spectrophotometer. Wafers, 15 mm in diameter, were prepared from 80 mg of zeolite under a pressure of 4 tons/cm^2. These samples were degassed for 2 h at 450 °C and 10^{-3} Torr; and the background spectrum was recorded after cooling to room temperature. The adsorption of pyridine (Merck, 99.5 wt%) was carried out at 150 °C, and the spectra were recorded in the 1700−1400 cm^{-1} range after desorptions at 150, 300, and 400 °C. The FTIR absorption bands at 1540 and 1450 cm^{-1} were associated with Brønsted and Lewis acid sites, indicating pyridinium ion and coordinated pyridine formation, respectively [31,32]. The TPD of pyridine was employed to quantify the acid sites strength and density. This analysis was performed on fresh, coked, and regenerated catalytic materials by desorption of preadsorbed pyridine from a saturator at 150 °C for 60 min, using N_2 as carrier gas. Before saturation with pyridine, the samples were pretreated at 400 °C for 1 h under a nitrogen atmosphere. The physisorbed pyridine was removed with a stream of nitrogen at a temperature of 150 °C for 1 h. Next, the samples were heated from an initial temperature of 150 °C following a heating ramp of 15 °C/min until reaching a final temperature of 780 °C. Finally, the desorbed pyridine was analyzed by chromatography with a FID detector.

The crystallographic properties were determined using a Siemens D500 X-ray diffractometer (XRD) with a CuKα monochromatic radiation source (λ = 1.5418 Å), data were collected in the 2θ range of 5–50°, with a step size of 0.05° and a dwell time of 3 s per step. The Si/Al atomic ratio in the structure of the zeolites was evaluated using the Breck-Flanigen correlation.

2.4. Catalytic evaluation tests

The conversion tests were conducted using a conventional Colombian VGO feedstock. Catalytic cracking experiments were carried out to assess the catalytic performance of zeolites with varying levels of intracrystalline mesoporosity and acidity. The chosen zeolites were named Y-0.00-S, Y-0.10-S, Y-0.20-S and Y-0.30-S. In order to evaluate the stability of the hierarchical zeolites and achieve the equilibrium state typical of equilibrated FCC catalysts, the coked zeolites (after cracking reactions) were regenerated *in situ* with an air current. After each regeneration cycle, the loss of activity of the zeolites was evaluated based on the conversion and selectivity of the different product groups. Four cycles of deactivation/regeneration were performed.

The experiments were carried out using a microactivity test (MAT) unit with a fixed-bed reactor by means of ASTM D-3907 standard. All conversion experiments were performed in triplicate, and the reported values represent the averages of these experiments. The Dixon test was utilized to analyze the data and exclude outliers, with confidence intervals set at the 95 % level. The reactions were performed at 550 °C, and the reaction times were 20, 30, 40 and 50 s. The mass of zeolite was 3.0 g, and the mass flow rate of VGO was 2.0 g min^{-1}. Both the feedstock and the amount of zeolite were kept constant, establishing the contact time as an operating variable, with the aim of varying the C/O ratio. Upon exiting the reactor, the reaction products were collected and subjected to analysis through gas chromatography, employing a Shimadzu GC-2014 chromatograph equipped with an FID detector. A non-polar column, 30 m in length and 250 μm in diameter, featuring a film thickness of 0.25 μm, was utilized for the chromatographic separation. Mass balances were greater than 95 % in all experiments in which the residence time in the stream was greater than 20 s. After each reaction and evacuation of the products, the zeolites are flushed with an N_2 stream for 20 min at the reaction temperature. The coke content on the zeolites after the reaction cycles was determined using temperature-programmed oxidation (TPO) method. Conversion was defined in the typical FCC context as the sum of the mass yields of dry gas (DG, C_1-C_2), liquefied petroleum gas (LPG, C_3-C_4), gasoline (C_5-216 °C), and coke fractions, each calculated as the ratio of the mass of the respective product to the mass of the feedstock.

2.4.1. Coke characterization

The coked zeolites were analyzed using techniques previously employed in other studies to identify the nature and composition of the coke produced by the reactions. Coke content was determined utilizing a temperature-programmed oxidation procedure. Carbon oxides (CO and CO_2) produced during combustion were transformed to methane in the presence of hydrogen using a Raney nickel catalyst and then quantified with an FID detector. The combustion profiles obtained provide information on the nature of the coke and its interaction with the active sites of the zeolite. In the case of the coked zeolites, the background FTIR spectra (*section* 2.3) allowed us to study the type of coke formed over each material. In this context, the signal at 1580 cm^{-1} was assigned to aromatic coke, while the signal at 1610 cm^{-1} was linked to olefinic coke. To study the composition of soluble coke, the coked zeolites were subjected to hydrofluoric acid (48 wt% in H_2O, ≥99.99 %) to detach the coking compounds from the porous structure. After by extraction with dichloromethane (ACS reagent, ≥99.5 %), the soluble coke was extracted and analyzed by gas chromatography. Coke extraction is a well-established method used to remove the zeolite structure and obtain a fraction soluble in CH_2Cl_2 [33].

2.4.2. Zeolite regeneration

The regeneration was carried out with air passage at a flow rate of 30 cm^3/min in an upward direction for 45 min at 570 °C to ensure that all the carbonaceous residue accumulated on the zeolite surface were burned. Finally, the zeolites regenerated in the last deactivation cycle were used to study their textural and acid properties.

Table 1
Feedstock properties. Colombian VGO.

°API	19.7
Aniline point (°C)	78.5
CCR (wt.%) [a]	0.43
Refractive index	1.4910
Distillation curve (°C) [b]	
Initial	272
10 vol %	387
30 vol %	420
50 vol %	450
70 vol %	487
95 vol %	534
Final	582
SARA fractions (wt. %) [c]	
Saturated	47.4
Aromatic	50.0
Resin	2.10
Asphaltene	0.50
Nickel (ppm)	0.48
Vanadium (ppm)	0.97
Sodium (ppm)	0.83
Iron (ppm)	0.24
Sulphur (wt. %)	1.12

[a] ASTM D-4530.
[b] ASTM D-1160.
[c] ASTM D-2007.

3. Results and discussion

3.1. VGO properties

The primary characteristics of VGO, which can be considered aromatic in nature, were shown in Table 1. With an API gravity of 19.7°, this feedstock was classified as heavy oil, as its value was below 22.3 [34]. This density may be associated with the elevated levels of aromatic hydrocarbons (50 wt%). The SARA fractionation in the VGO is useful for predicting a commercial unit's yields. Some authors have studied the correlation between the SARA composition of a VGO with the products obtained and found that a higher content of aromatic species favors the yield of aromatic gasoline with high RON values [35–37]. As could be seen in Table 1, the aromatic fraction represented 50.0 wt% in VGO, thus confirming its aromatic nature; the next most prevalent fraction was the saturated hydrocarbons, with a concentration of 47.4 wt%, followed by the resin with 2.10 wt%, and the trace presence of asphaltenes at just 0.50 wt%. The simulated distillation curve showed that 10 % of the hydrocarbons are distilled at 387 °C and 95 % at 534 °C, which also aligns with its API density.

3.2. Zeolites properties

The properties of zeolites are decisive in catalytic processes given the set of consecutive stages that take place: diffusion through the pores, adsorption of the reactant on the active center, chemical reaction, desorption of the product, and diffusion of the same through the channels, which affects the activity and final selectivity of the zeolite. The crystalline and textural properties of the fresh zeolites used in this research are shown in Table 2. The alkaline desilication treatment altered the porosity of the zeolites, resulting in increased mesoporosity in the materials subjected to more severe treatments. The most important differences in textural properties were observed in the mesopore volume, specific surface area and average mesopore diameter. Zeolite Y-0.20-S presented the highest mesopore-specific surface area while zeolite Y-0.00-S had the lowest value. Regarding the average mesopore diameter, the zeolites Y-0.20-S and Y-0.30-S presented the highest values. This substantial improvement in the mesoporosity of the treated zeolites became a positive aspect of facing the diffusive problems that could occur during catalytic cracking. A negative aspect of the use of high concentrations of alkali (NaOH solution >0.20 M) is the excessive loss of crystallinity. In the case of the zeolite with the highest alkaline treatment (Y-0-30-S), it suffered a loss of crystallinity of 60 % as a consequence of the destabilization of the crystalline network. As expected, this loss of crystallinity in the Y-0.30-S zeolite was accompanied by a reduction in strong Brønsted acid sites (approximately 11 %), which are typically located within the micropores of the zeolite.

An important property of this zeolite type is its acidity (nature, concentration, and strength), due to the carbocationic reaction mechanism that drives these chemical processes, as well as its impact on activity and selectivity [38]. Table 3 shows the distribution of acidic sites in the zeolites (nature, Brønsted, and Lewis and acid strength, weak and strong). The density of Brønsted acid sites depends on the amount of aluminum present in the crystal network; in this sense, the number of Brønsted sites will be proportional to the concentration of aluminum. Instead, extra-framework aluminum species give rise to Lewis acid sites. The alkaline treatment is selective in the removal of silicon from the network, so a significant decrease in the B/L ratio would be expected. However, it was observed that the zeolites Y-0.10-S and Y-0.20-S maintained their constant B/L ratio as a consequence of possible removal of aluminum from the crystalline network in addition to the remission of silicon. For these two zeolites, this behavior was evidenced by the increase in the concentration of Lewis sites given to the possible presence of extra-framework aluminum.

All zeolites showed increased acidity, as indicated by the quantity of pyridine that remained adsorbed following desorption at 150 °C, compared to the parent zeolite (Y-0.00-S). Removing silicon from the network clearly explained the increase in Brønsted sites. However, the increase in Lewis sites was explained by the leaching of part of the aluminum from the network and its deposition as an amorphous material, forming part of the aluminum species with an acid character. Of the four zeolites characterized, Y-0.20-S had the greatest concentration of total acid sites (209 μmol Py/g, desorption at 150 °C), while zeolite Y-0.30-S had the highest concentration of strong acid sites (67 μmol Py/g, desorption at 400 °C).

Table 2
Crystalline and textural properties of the fresh zeolites after steaming.

	Y-0.00-S	Y-0.10-S	Y-0.20-S	Y-0.30-S
Textural properties				
BET specific surface area (m^2/g)	712	622	614	473
Micropore specific surface area (m^2/g)	501	315	248	162
Mesopore specific surface area (m^2/g)	211	307	366	311
Total pore volume (cm^3/g)	0.533	0.611	0.636	0.652
Micropore volume (cm^3/g)	0.267	0.242	0.133	0.140
Mesopore volume (cm^3/g)	0.266	0.369	0.503	0.512
Average mesopore diameter (Å)	53.1	59.5	67.2	84.7
Crystalline properties				
Crystallinity (%)	99	65	61	40
Unit cell size (Å)	24.26	24.28	24.29	24.30
Si/Al in the framework	31.0	26.4	25.9	23.7

Table 3
Concentration of Brønsted (B) and Lewis (L) Acid Sites (μmol Py/g) from FTIR experiments in fresh zeolites after steaming.

Samples	150 °C			300 °C			400 °C		
	B	L	B/L	B	L	B/L	B	L	B/L
Y-0.00-S	108	72	1.5	73	48	1.5	35	24	1.5
Y-0.10-S	106	88	1.2	79	69	1.1	27	19	1.4
Y-0.20-S	116	93	1.2	85	71	1.2	31	22	1.4
Y-0.30-S	116	68	1.7	55	62	0.9	31	36	0.9

3.3. Conversion

The catalytic performance of the hierarchical zeolites was evaluated under experimental conditions adjusted according to the objectives set out in this work in a MAT reactor (*see section* 2.4). Some authors have studied hierarchical zeolites in the catalytic cracking of VGO. However, it had only been done during a single cycle without including its regeneration and stabilization [39–41]. The importance of this research was to study the stability of zeolites through several deactivation/regeneration cycles until reaching the typical equilibrium of equilibrated FCC catalysts. Commercial catalysts employed in catalytic cracking processes are formulated (porosity and acidity) according to the nature of the charge to be processed and the refinery's production objectives. Knowing the reactivity of VGO against equilibrated zeolites would help to understand and predict the impact of its composition on the distribution of products and their deactivation.

In the FCC process, the zeolites are subjected to very severe cyclical processes, having to circulate between the reaction zone and the regeneration zone, which could produce important changes in their structure due to the permanent variations of the environmental conditions to which they are subjected. Therefore, it is essential to study the stability of these materials through several deactivation/regeneration cycles [42]. Fig. 1 shows the conversion of VGO during four deactivation/regeneration cycles, as a function of reaction time on hierarchical zeolites at 550 °C. This figure illustrates the conversion of the zeolites Y-0.00-S (Fig. 1a), Y-0.10-S (Fig. 1b), Y-0.20-S (Fig. 1c) and Y-0.30-S (Fig. 1d). The conversion curves obtained allowed us to determine the number of reaction cycles necessary for the zeolites to reach catalytic equilibrium (equilibrated zeolites). It was observed that after the third reaction cycle, the zeolites reached equilibrium, with similar conversions in the last two reaction cycles. In general, zeolites with lower mesoporosity (mesopore volume and average mesopore diameter) suffered greater activity losses with each deactivation/regeneration cycle, reaching conversion losses between the first cycle and the last cycle at short times of up to 30 wt% in zeolite Y-0.00-S. Another

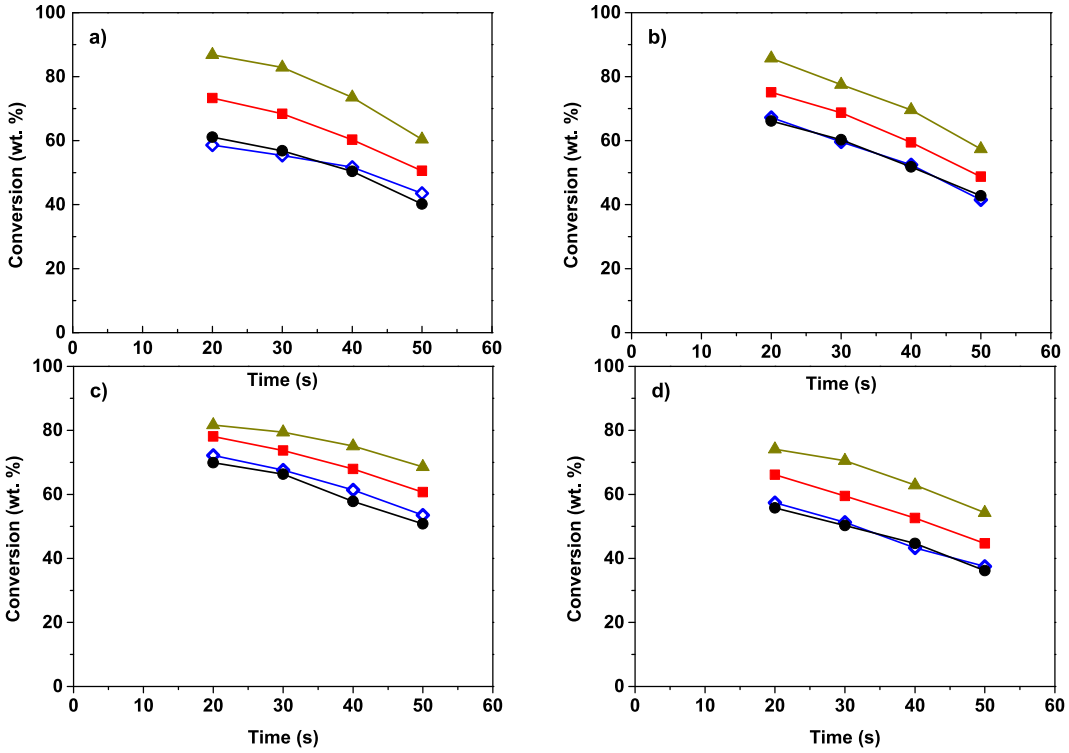

Fig. 1. VGO conversion at 550 °C as a reaction time function over hierarchical zeolites: (a) Y-0.00-S, (b) Y-0.10-S. c) Y-0.20-S and d) Y-0.30-S. Symbols: *triangles*, cycle 1; *squares*, cycle 2; *open diamonds*, cycle 3; ●, cycle 4.

important aspect of zeolite Y-0.00-S was the presence of strong acid sites (30 % of its total acidity), which could have favored a strong interaction with basic products (such as aromatic species) and deposited strongly on their active sites, thus causing a greater impact on their conversion with each reaction cycle. In contrast, the zeolite that suffered the least impact on its conversion with the reaction cycles was Y-0.20-S, with losses of up to 14 wt%.

In the first reaction cycle, it was observed that the zeolites Y-0.00-S and Y-0.10-S showed the maximum conversions at short times, with values above 80 wt%, typical of FCC industrial processes. These high conversions could have been favored by a confinement effect in the microporous channels of these zeolites, where the adsorbed molecules tended to strengthen their van der Waals interactions. The strong field gradients present within the microporous channels of zeolites cause a contraction of the orbitals of the molecules contained in these channels and cavities. This contraction alters the energy levels, resulting in an increase of the energy of the boundary orbitals, which subsequently pre-activates the reacting molecule. Consequently, the confinement effect increases the strength of the acid sites, thus favoring the cracking reactions [43].

3.4. Product yields

Figs. 2 and 3 show the gas yield curves for VGO during deactivation/regeneration cycles on hierarchical zeolites at 550 °C. These figures illustrate the dry gas (Fig. 2) and LPG (Fig. 3) yields through four reaction cycles: cycle 1 (Figs. 2I and 3(I)), cycle 2 (Fig. 2(II) and 3(II)), cycle 3 (Fig. 2(III) and 3(III)) and cycle 4 (Fig. 2(IV) and 3(IV)). It was seen that the gases were stable primary products whose yields increased with conversion, a fact typical of the formation of gases in the catalytic cracking of hydrocarbons [4]. Also, it is observed that at high conversions, the gases are secondary products. Their production increases more rapidly, reflecting the contribution of overcracking heavier fractions, which leads to the formation of lighter hydrocarbons within the gas range. This behavior is characteristic of VGO in FCC commercial units, whose catalytic activity is usually associated with greater gas production [44,45].

Zeolite Y-0.00-S showed the highest selectivity to dry gas, while zeolite Y-0.30-S showed the lowest value. This behavior corresponds to the higher conversion observed, associated with higher gas production. As the deactivation/regeneration cycles advanced, a decrease in gas production was observed. In the production of LPG, the difference between zeolites was minimal, observing a greater difference between reaction cycles. Table 4 shows the selectivity and olefinicity values of the LPG cut at an approximate conversion of

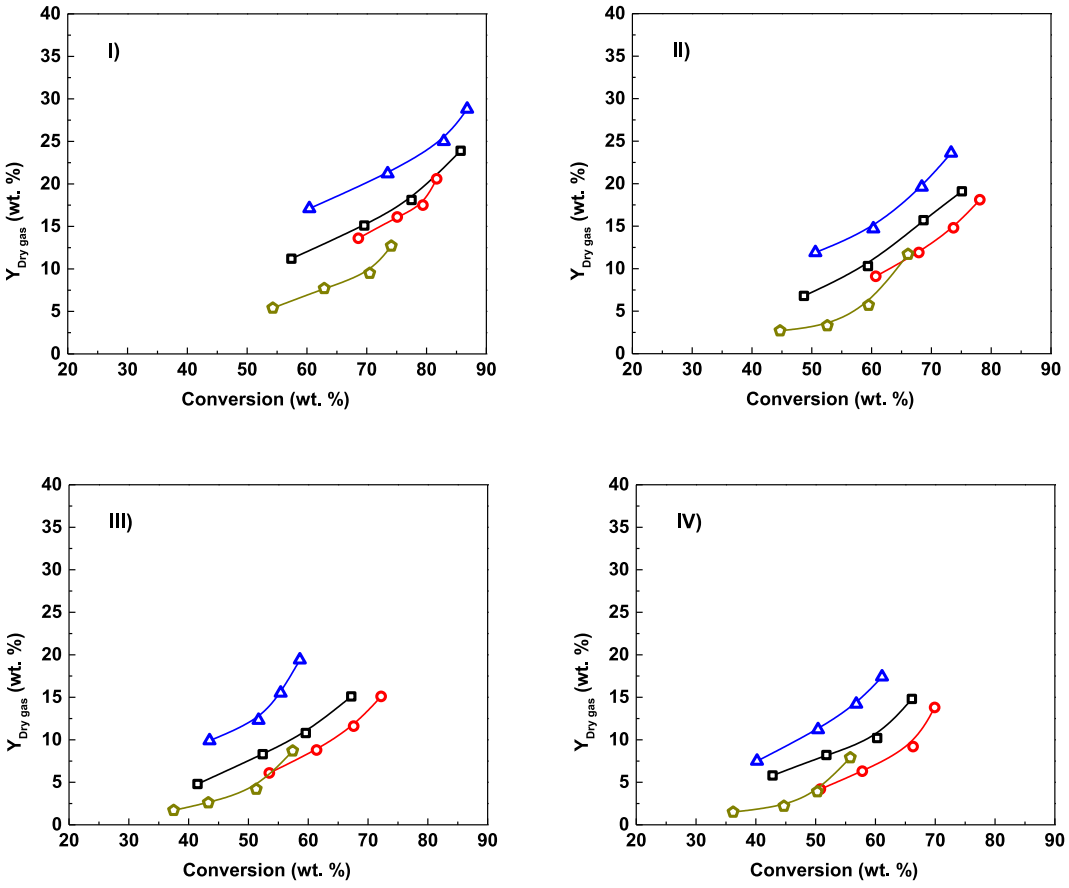

Fig. 2. Dry gas yields as a function of the conversion of VGO (Four reaction cycles). (**I**) *Cycle 1*, (**II**) *Cycle 2*. (**III**) *Cycle 3* and (**IV**) *Cycle 4*. Symbols: *triangles*, Y-0.00-S; ***squares*, Y-0.10-S**; *circle*, **Y-0.20-S**; *pentagons*, Y-0.30-S.

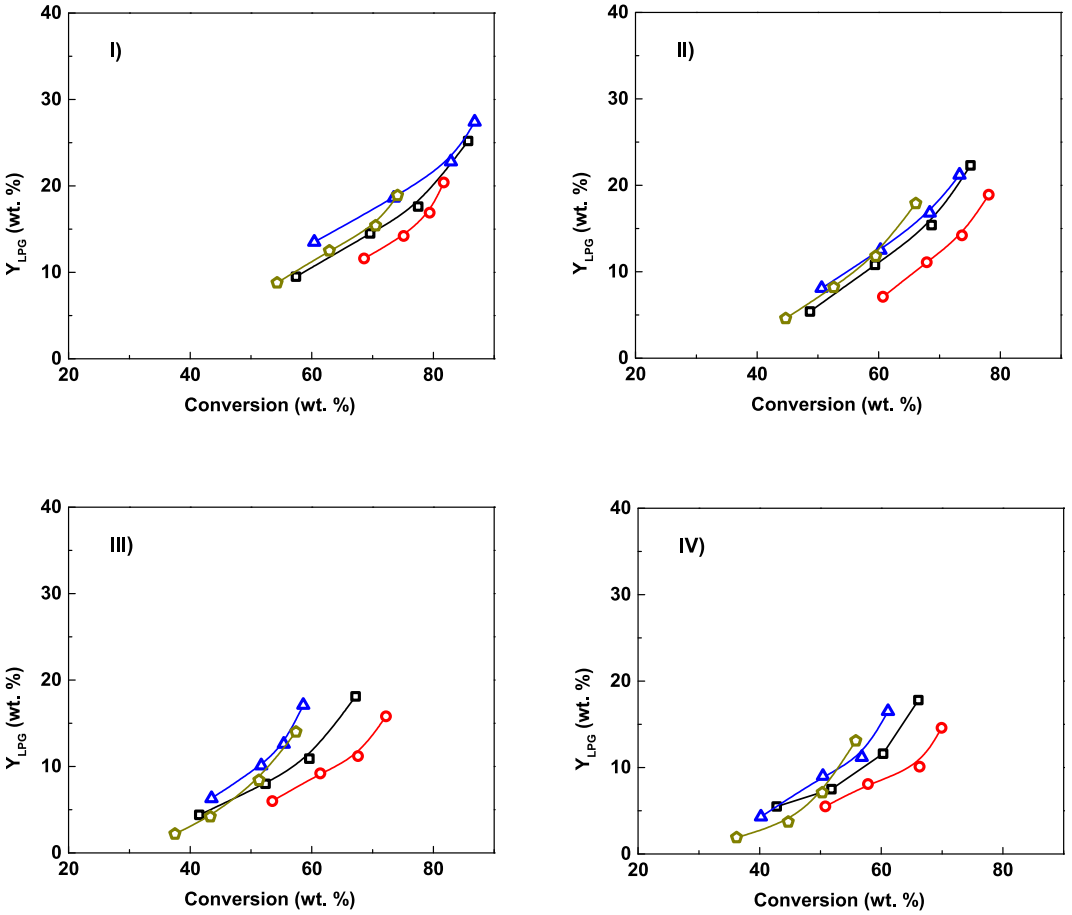

Fig. 3. LPG yields as a function of the conversion of VGO (Four reaction cycles). (**I**) *Cycle 1*, (**II**) *Cycle 2*. (**III**) *Cycle 3* and (**IV**) *Cycle 4*. Symbols: *triangles*, Y-0.00-S; *squares*, Y-0.10-S; *circle*, Y-0.20-S; *pentagons*, Y-0.30-S.

60 wt%. The selectivities at LPG cut presented the same trends observed in Fig. 3, with zeolite Y-0.00-S presenting the highest value. Within the LPG cut, the presence of olefins is important, given its usefulness as a raw material in the petrochemical industry. The olefinicity, expressed as the ratio of the productions ($C_3 = + C_4 =$)/(GLP), was close between zeolites for the same reaction cycle, with a significant increase observed between the first (cycle 1) and the last cycle (cycle 4). Given the lower Brønsted acidity in the re-generated zeolites (*see* Table 8), the olefinicity of C_3-C_4 hydrocarbons was higher in the last cycle for all zeolites, indicative of a lower incidence of hydrogen transfer reactions known to consume olefins and naphthenes to produce paraffins and aromatics [46].

The gasoline cut was the most important within the group of hydrocarbons produced during catalytic cracking. Therefore, any positive variation in its production and quality could represent great economic benefits. This cut comprised a wide variety of hydrocarbons in the C_5-C_{12} range, and its quality as fuel was expressed as a function of the RON octane number. Fig. 4 shows the yield curves for gasoline as a function of the conversion of VGO. This figure presents the gasoline production for the four reaction cycles: cycle 1 (Fig. 4I), cycle 2 (Fig. 4(II)), cycle 3 (Fig. 4(III)) and cycle 4 (Fig. 4(IV)). The gasoline production curves showed linearity in a wide conversion range (increased with conversion), typical of primary products. However, at high conversions, it could be over-cracked to give lighter products such as dry gas or LPG. Thus, the gasoline cut could be defined as an unstable primary product [47,48].

Comparing zeolites and between each deactivation/regeneration cycle, zeolite Y-0.20-S showed the best gasoline yields, reaching values of up to 35 wt%, which were close to the values typically obtained in refineries. Another outstanding aspect was the stability

Table 4
Selectivity and olefinicity of LPG cut. Conversion approximately 60 wt%).

	First cycle (1)				Last cycle (4)			
	Y-0.00-S	Y-0.10-S	Y-0.20-S	Y-0.30-S	Y-0.00-S	Y-0.10-S	Y-0.20-S	Y-0.30-S
S_{GLP} (% *p/p*)	22.5	15.8	19.3	20.0	19.0	19.1	17.3	21.2
$(C_3 = + C_4^=)$/GLP	20.2	22.1	22.7	23.9	23.9	23.0	27.3	29.4

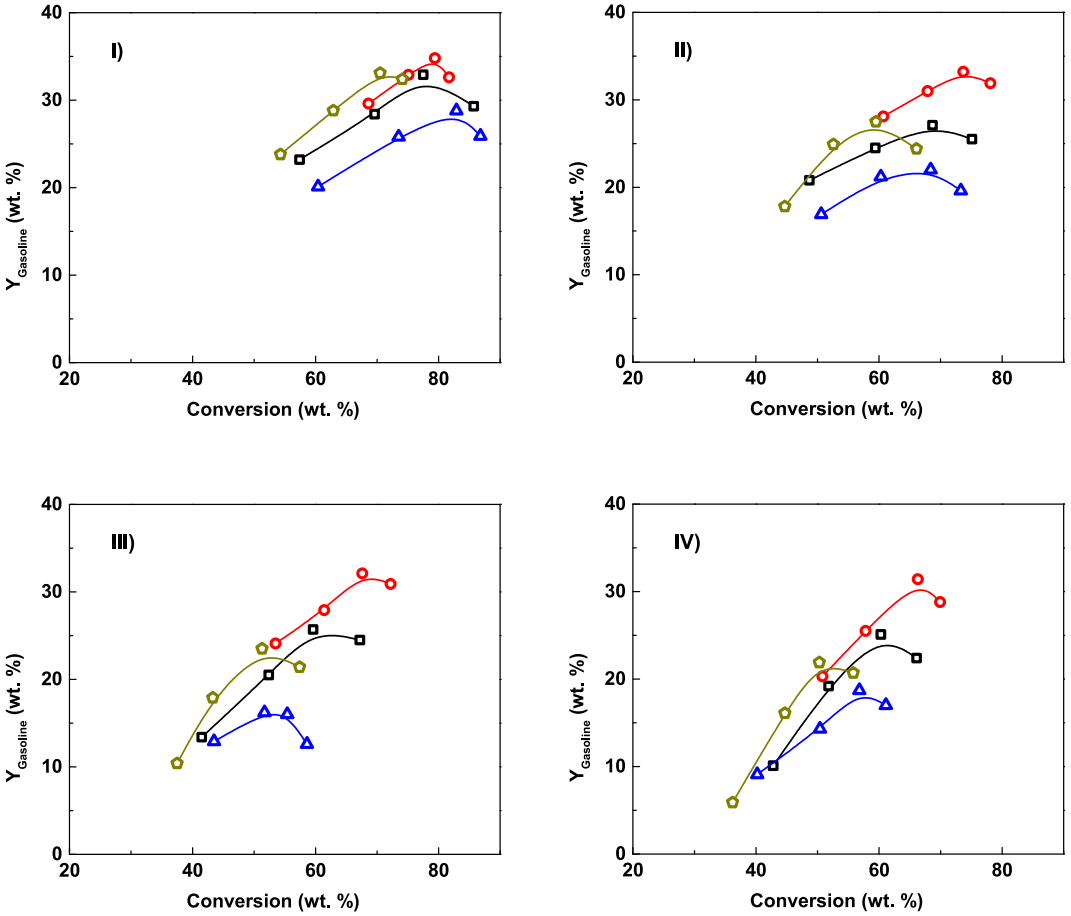

Fig. 4. Gasoline yields as a function of the conversion of VGO (Four reaction cycles). (**I**) *Cycle 1*, (**II**) *Cycle 2*. (**III**) *Cycle 3* and (**IV**) *Cycle 4*. Symbols: *triangles*, Y-0.00-S; *squares*, Y-0.10-S; *circle*, Y-0.20-S; *pentagons*, Y-0.30-S.

shown by this zeolite, which even during the fourth reaction cycle continued to show conversion values above 65 wt%. This greater selectivity towards the gasoline cut was favored by its greater mesopore-specific surface area and high average mesopore diameter, which favored the formation of hydrocarbons and their rapid diffusion in the gasoline range (C_5-C_{12}). The mesopores generated in hierarchical zeolites functioned similarly to the matrix in FCC catalysts. The matrix typically possesses a macro and mesoporous structure, enabling the precracking of bulky hydrocarbon molecules. This precracking reduces the size of the molecules, generating intermediate products. Based on the results obtained, this zeolite would have been useful in synthesizing a commercial catalyst to maximize the production and amount of gasoline cut.

The quality of the gasoline cut expressed as a function of the octane index is related to the concentration of the different groups of hydrocarbons that compose it, influenced by the properties of the catalyst, the characteristics of the feed, and the reaction conditions. The distribution of hydrocarbons and quality in the gasoline boiling range is shown in Table 5. It was possible to show that the composition and quality of the gasoline cut were related to the properties of the zeolites, in this sense the zeolite Y-0.20-S presented the highest concentration of olefinic and aromatic gasoline, which was reflected in higher RON values. The RON values obtained with the other zeolites were low in relation to those obtained in commercial gasoline (usually greater than 90). The main source of aromatics are

Table 5
Composition and quality of the Gasoline cut. Conversion approximately 60 wt%).

	First cycle (1)				Last cycle (4)			
	Y-0.00-S	Y-0.10-S	Y-0.20-S	Y-0.30-S	Y-0.00-S	Y-0.10-S	Y-0.20-S	Y-0.30-S
Paraffins	31.3	27.5	7.5	14.9	32.5	30.4	10.3	16.4
Olefins	21.1	23.8	32.1	30.2	20.6	23.0	29.5	27.8
Naphthenes	27.9	21.3	15.5	23.5	29.2	19.8	21.5	25.8
Aromatics	19.7	27.4	44.9	31.4	17.7	26.8	38.7	30.0
RON	81	83	92	88	78	79	90	86

dealkylation reactions of aromatic molecules present in the feed, through which compounds with molecular weights in the gasoline range can be formed [49]. These values obtained from aromatics in gasoline, for zeolites Y-0.20 and Y-0.30-S in the range between 20 and 45 wt%, correspond to the typical percentages obtained in the refinery that are usually in the selectivity range of 20–40 wt% [50]. The lower tendency to form aromatics of the zeolites Y-0.00-S and Y-0-10-S could be justified due to their lower mesoporosity, which hinders the diffusive transport of molecules with larger kinetic diameters. Thus, these molecules would be less involved in secondary reactions such as hydrogen transfer, which would lead to a greater formation of aromatic species [51].

Comparing the first and the last cycle, it was observed that the composition of the gasoline cut was similar throughout the cycles, with a higher concentration of paraffinic gasoline in the Y-0.00-S and Y-0.20-S zeolites, and olefinic and aromatic in the Y-0.20-S and Y-0.30-S zeolites. The greater selectivity to paraffin gasoline in the zeolites with greater microporosity was due to the direct cracking of the long paraffin chains that, given their high reactivity, could adsorb on the catalytic sites and undergo conventional β cracking and hydrogen transfer reactions, which originated new paraffins in the gasoline range [52].

3.4.1. Coke

The coke accumulated on the surface of the zeolites used in cracking processes is primarily responsible for their rapid and reversible deactivation. At the same time, it plays a crucial role in the process by acting as the heat source needed to sustain the chemical reactions in the vertical reactor while burning in the regenerator. The characteristics of the feed, the operating conditions, and the catalyst's properties determine the coke's performance and characteristics. Hydrocarbons mainly comprised of species with high molecular weights and condensed aromatic structures are regarded as the primary precursors for coke formation in catalytic cracking processes. These species generally have high carbon conradson (CCR) values related to the coking potential of a given hydrocarbon fraction.

The coke yield was calculated by integrating the areas under the curves of the TPO profiles of the coked zeolites. (*see* Fig. 5). Table 6 shows the coke selectivities obtained in different catalytic cracking cycles of VGO on hierarchical zeolites. It was observed that the coke production increased with each cycle, presenting the highest values in the last reaction cycle (cycle 4). The zeolites with the highest mesoporosity, such as Y-0-20-S and Y-0.30-S, showed the highest coke selectivities with values ranging mostly between 20 and 35 wt %. This increase in coke production of zeolites with higher intracrystalline mesoporosity generated by alkaline treatment has been previously observed by other authors in the cracking of feedstocks such as VGO, ATR-VGO, and bio-oil, which has been ascribed to the increased volume of free space in mesoporous cavities [53]. The greater volume of mesopores generated by the alkaline treatment allows coke precursors to be more easily accommodated, which in the presence of a high density of acid sites, favor alkylation, oligomerization, hydrogen transfer, cyclization and condensation reactions that lead to the formation of carbonaceous deposits [54,55]. Even though the Y-0.20-S zeolite showed high selectivity for coke production, it maintained a high activity in the production and quality of gasoline, compared with the zeolites with higher microporosity.

An important aspect is its high resistance to deactivation by coke formation through the reaction cycles, a behavior also observed by other authors in the gasoline production process from methanol, who attributed it to the interconnectivity between the intracrystalline mesopores, which prevents the blockage of pores by carbonaceous depositions [56,57]. The slower rate of deactivation is also ascribed to the enhanced and more consistent accessibility of acid sites resulting from the incorporation of mesopores in zeolite Y-0.20-S [58]. It's also reported in previous studies about the reduced deactivation of mechanochemically delaminated hierarchical zeolite MCM-22 catalysts during 4-propylphenol cracking [59]. This effect is attributed to a combination of accessible active sites and effective pore confinement. Thus, a balance must be maintained between increasing mesopore volume and preserving catalytic activity by keeping

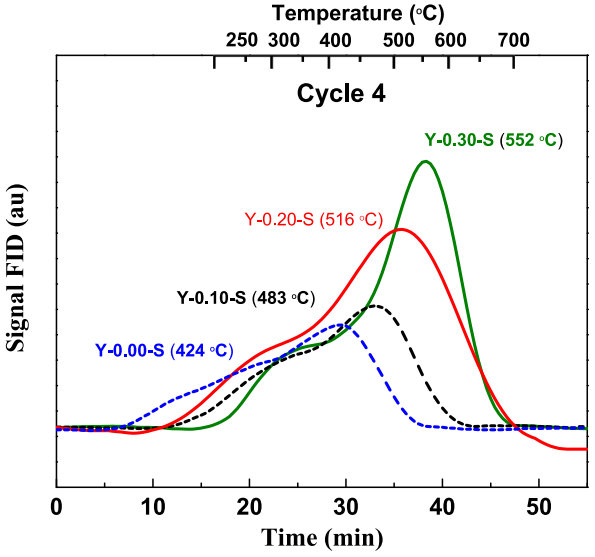

Fig. 5. TPO profiles of the coke combustion deposited on the spent catalyst at VGO conversion at about 75 %. First Cycle (1) and Last Cycle (4).

Table 6
Coke selectivities in the catalytic cracking of VGO on hierarchical zeolites. (Conversions approximately 60 wt%).

Cycle	Y-0.00-S	Y-0.10-S	Y-0.20-S	Y-0.30-S
1	10.75	16,67	20,12	22,10
2	14,62	15,28	15,60	24,37
3	16,21	20,47	18,79	29,63
4	16,69	22,22	30,97	34,59

acid sites within pores of optimal size. Another important factor is the difference between the size of the cages where coke forms and the pore openings of these cages. If large cages, where coke formation is favored, are only accessible through small pores, the stereochemical blockage effect is significant, leading to pronounced deactivation. These zeolites with greater microporosity are described as having trapping cages [57]. This factor accounts for the difference observed in the deactivation rates of the Y-0.00-S and the Y-0.20-S zeolites. Furthermore, it was observed that the deactivation was faster in the Y-0.00-S zeolite compared to the hierarchical zeolites. During the deactivation/regeneration cycles, zeolite Y-0.00-S exhibits the most significant increases in coke selectivity, with increments reaching up to 62 % in the final reaction cycle. These results suggest that zeolites with greater microporosity have coke trapping cages, leading to a progressive loss of activity even after only a few reaction cycles.

Fig. 5 shows the combustion profiles of the coke generated from VGO in the last reaction cycle on zeolites, with the conversion being approximately 60 wt%. A main peak was observed in all combustion profiles at temperatures higher than 400 °C. For the Y-0.20-S and Y-0.30-S zeolites, the peak was located between 500 and 550 °C, while for the Y-0-00-S and Y-0.10-S zeolites, it was between 400 and 500 °C. Additionally, in some cases, a low-intensity peak was observed at temperatures below 400 °C. The differential behavior in coke combustion is a result of its varying difficulty to burn, which can be attributed to the composition of the coke. The peak at low temperatures (<400 °C) is associated with coke composed of compounds that have undergone minimal condensation, such as aliphatic and aromatic species with an elevated H/C ratio. Conversely, the peak observed at high temperatures (>500 °C) refers to compounds with a greater degree of condensation (low H/C ratio), comprising condensed dienes and aromatic structures.

The observed behavior in the combustion profiles aligns with the findings from the analysis of coke nature conducted using FTIR (refer to Table 7). In this FTIR characterization of coke, Y-0.20-S and Y-0.30-S zeolites exhibited the most pronounced presence of aromatic coke (band at 1580 cm-1). When this is correlated with the elevated combustion temperatures observed in the TPO, it suggests that the coke possesses a strong basic character (low H/C ratio), consequently leading to robust interaction with the acid sites of the zeolites. This second type of coke forms within the zeolite micropores; however, due to its high degree of condensation, it is believed that its further growth is encouraged outside the zeolite crystals [60]. The higher mesoporosity of the zeolites promotes the formation of this type of coke, facilitating its growth and condensation. FTIR analysis identified the presence of two distinct types of coke on all zeolites, with the olefinic nature being predominant on zeolite Y-0.00-S (band at 1610 cm^{-1}).

Coke extraction is a known procedure to destroy the structure of zeolites to obtain a fraction soluble in CH_2Cl_2 that allows to identification of the coke deposited in the material [61]. Given the conditions under which the catalytic cracking was carried out, the soluble coke is likely to be trapped within the microporous structure of the spent zeolite. The carbonaceous deposits were first removed from the zeolite by dissolving the aluminium and silicon matrix in a HF solution at room temperature. Next step, CH_2CL_2 is used to extract the soluble compounds and the non-soluble compounds are obtained by filtration. Guisnet et al. showed that carbonaceous substances do not undergo any chemical changes due to treatment with the acid solution [60].

Fig. 6 presents the primary compounds identified in the soluble coke fraction of the coked zeolites. These compounds predominantly include aromatic species with one, two, three, and four rings, designated A1, A2, A3 and A4, respectively. It was found that the zeolites with the highest mesoporosity (Y-0.20-S and Y-0.30-S) showed a significant presence of aromatic species with a higher degree of condensation. In particular, Y-0.20-S presented a composition with a ratio of 70 % by weight of A4 + A3 and 30 % by weight of A1 + A2. On the other hand, for zeolite Y-0.30-S, the ratio was 82 wt% of A3 + A4 and 18 % wt% of A1 + A2.

In contrast, the zeolites with greater microporosity showed species with a lower degree of condensation. The composition of the soluble coke fraction for Y-0.00-S was 60 % by weight of A1 + A2 and 40 % by weight of A3 + A4. Meanwhile, zeolite Y-0.10-S presented a composition with a ratio of 52 % by weight of A1 + A2. Previous studies have shown that coke molecules are formed inside the zeolite pores where most acid sites are located [61]. As a result, the growth of coke molecules is limited by the size of the cages or channels; therefore, for identical conversions, the coke yield is lower in zeolites with higher microporosity and their composition shows a lower degree of condensation. These results are in agreement with what has been observed in the combustion profiles and in the characterisation of the coke by FTIR.

Table 7
Intensities of the FTIR Bands Assigned to Aromatic Coke (1580 cm−1) and Olefinic Coke (1610 cm−1) formed after the last deactivation cycle (Cycle 4). Conversion approximately 60 wt %.

Signal	Y-0.00-S	Y-0.10-S	Y-0.20-S	Y-0.30-S
Aromatic band (1580 cm^{-1})	2.00	3.10	4.68	6.90
Olefinic band (1610 cm^{-1})	3.20	2.00	2.50	2.40

Table 8
Textural properties of the fresh, coked, and regenerated zeolites after the last deactivation cycle (cycle 4). Conversion approximately 60 % wt.

	Y-0.00-S			Y-0.10-S			Y-0.20-S			Y-0.30-S		
Textural properties	fresh	coked	regen	fresh	coked	regen	fresh	coked	regen	fresh	coked	regen
SBET (m^2/g)	712	441	506	622	298	391	614	379	510	473	215	341
SMicropore (m^2/g)	501	263	304	315	137	186	248	172	203	162	149	102
Smesopore (m^2/g)	211	178	202	307	161	205	366	207	307	311	66	239
Total PV (cm^3/g)	0.533	0.382	0.416	0.611	0.299	0.432	0.636	0.358	0.522	0.652	0.371	0.563
Vmicropore (cm^3/g)	0.267	0.150	0.195	0.242	0.106	0.198	0.133	0.157	0.123	0.140	0.167	0.114
Vmesopore (cm^3/g)	0.266	0.232	2.221	0.369	0.193	0.234	0.503	0.201	0.399	0.512	0.204	0.449
Average mesopore diameter (Å)	53.1	22.4	36.7	59.5	32.1	40.3	67.2	36	59	84.7	42.1	63.5

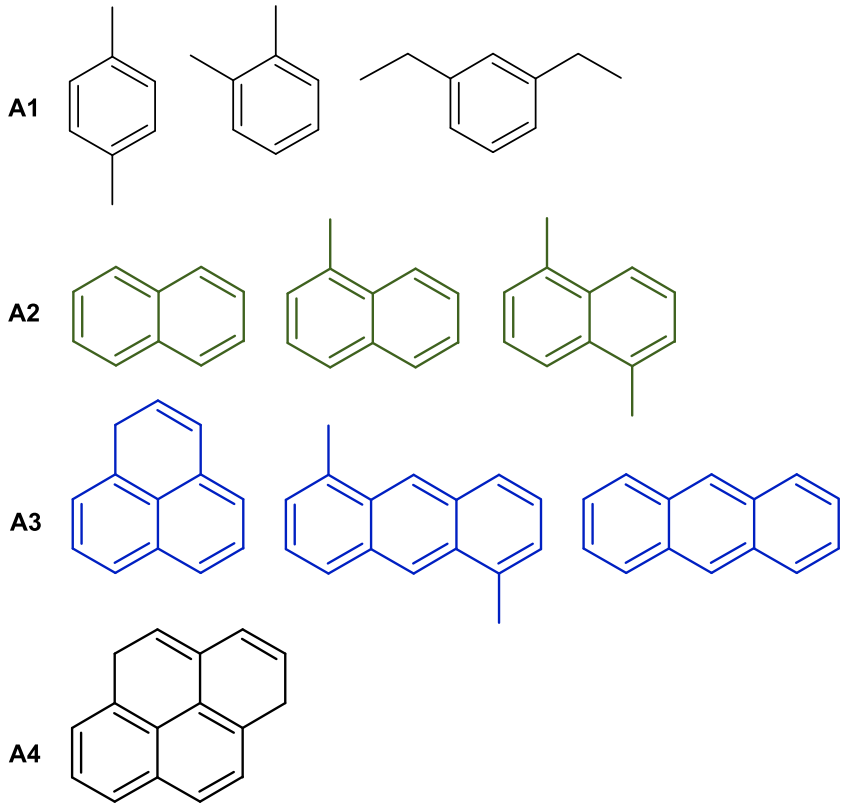

Fig. 6. Main compounds identified and quantified in the soluble coke fraction after the fourth reaction cycle.

3.4.2. Textural properties of the fresh, deactivated, and regenerated zeolites

The coked zeolites, after four reaction cycles and subsequent regeneration in an air stream for 45 min at 570 °C, were extensively characterised to assess the effect of deactivation and regeneration cycles on their properties. Table 8 shows the textural properties of the fresh, coked, and regenerated zeolites at the same conversion. As mentioned, the fresh zeolites present a porosity constituted mainly by micropores in the parent zeolite (Y-0.00-S) and mesopores in the modified zeolites. In Y-0.00-S, the total pore volume is 50 % composed of micropores, while in modified zeolites the values decrease significantly, reaching as low as 20 %. Expectedly, it was observed in all cases (coked and regenerated zeolites) that both the pore volumes (total volume, micro and mesopore) and the areas BET (surface area, micro and mesopore) decreased in comparison to the fresh zeolites. In addition, the average mesopore sizes were reduced in the coked zeolites, indicating partial pore blocking.

Despite the lower coke selectivity observed with the Y-0.00-S and Y-0.10-S zeolites, the impact on their textural properties was higher. The BET-specific surface reached losses of up to 52 % in the zeolite Y-0.10-S, mainly affecting micropore micropore-specific surface area. On the other hand, the zeolites with the highest mesoporosity, which also showed higher selectivities to coke, suffered the least impact on their BET area. Regarding the pore volume in the coked zeolites, it was observed that those with higher mesoporosity experienced a slight increase in their micropore volume compared to fresh zeolites. This phenomenon could be attributed to coke deposition in the mesopores, leading to the formation of new micropores. It has been postulated that coke develops outside the zeolite crystals, specifically in the intracrystalline mesopores, and that the partial blockage of these mesopores by coke

could result in the creation of new micropores [56]. In this sense, the significant impact could be due to the high percentage of mesopores present in the fresh zeolites Y-0-20-S and Y-0.30-S, which contain up to 79 % mesopores. Therefore, the partial blockage of the mesopores in the coked zeolites could lead to a noticeable increase in their micropore volume. These results are consistent with the observed changes in the average mesopore diameter, where the coked zeolites Y-0.20-S and Y-0.30-S reduced their diameters by up to 54 %, compared to a 40 % reduction in Y-0.00-S. In general, the average diameter of the mesopores followed the same trend as other properties, with zeolite Y-0.20-S showing the best performance in terms of regeneration, maintaining almost 90 % of its initial value. Regeneration of the zeolites restored much of the original surface area and porosity, demonstrating the effectiveness of this treatment in removing most of the coke deposits. This different behaviour in the regeneration of the coked zeolites can be attributed to the different degrees of difficulty of coke combustion, which are influenced by the different degrees of mesoporosity of the Y zeolites. A higher mesoporosity could facilitate the access of combustion air, and thus favor the total burning of the coke that releases the active sites of the material.

3.4.3. Acidity of the coked and regenerated zeolites

Table 9 shows the amount of total acidity and acid site distributions ($\mu mol_{Py}/g$) in fresh, coked, and regenerated zeolites after the last deactivation cycle. As expected, the acidity of all the coked zeolites was reduced compared to the fresh ones, with losses exceeding 40 % in most cases, except for zeolite Y-0.30-S, which showed a more significant reduction of 60 %. Although zeolite Y-0.30-S experienced the most significant impact on its acidity due to its high coke selectivity, it is evident that after regeneration, it readily removed carbonaceous residues, thus recovering a significant portion of its acidity. The higher impact of coke on zeolite Y-0.30-S could be due to its high mesoporosity and acidity (which includes more Brønsted acid sites and a higher concentration of strong acid sites), as opposed to the presence of molecules with resonant structures and high electronic density (basic character), which promote condensation reactions leading to the formation of more and larger coke deposits. The order of coke selectivities at approximately at an approximately similar conversion (60 wt%) was: Y-0.30-S > Y-0.20-S > Y-0.10-S > Y-00-S.

The acid sites present in Y zeolites can interact differently concerning basic molecules and selectively direct the production of products. Brønsted sites play a greater role in the propagation of cracking reactions than Lewis sites [62]. Table 9 demonstrates that zeolites subjected to coking after the last deactivation cycle undergo a preferential decrease in the percentage of Brønsted acid sites. Previous studies have indicated that Lewis acid sites within the zeolites composing FCC catalysts tend to remain more concealed within the zeolitic structure [63]. In addition, deactivation during the catalytic cracking process is attributed to the dehydroxylation of Brønsted acid sites, which are critical for the catalytic reaction. Following dehydroxylation, the system transitions to a metastable state in which aluminium is readily released from the zeolite framework, forming extra-framework aluminium (EFAL) species that create new Lewis sites. In this context, the relatively greater decline in Brønsted sites across both catalysts could stem from enhanced accessibility of these molecules present in each feed to the Brønsted sites, favoring dehydroxylation reactions and greater coke formation at these sites. Regarding regeneration, it is noted that despite a reduction in acidity, the proportion of Brønsted and Lewis sites maintains a consistent pattern as observed in fresh zeolite, affirming the effectiveness of the regeneration process.

As for the acid strength, calculated from the TPD-Py profiles, as expected, a higher proportion of weak acid sites prevails in coked zeolites, which could be due to the initial predominance of weak acid sites. Strong character in fresh zeolite, which adsorb them more strongly in the presence of basic compounds such as coke deposited on the zeolite. In general, the *in situ* regeneration of these zeolitic materials manages to recover the catalytic activity, preserving even after four deactivation/regeneration cycles in all cases its acidic and textural properties.

4. Conclusions

The thermal stability of hierarchical zeolites was studied through multiple deactivation/regeneration cycles using a MAT type fixed bed reactor. This multicyclic study allowed us to simulate the reaction conditions that these materials must face on an industrial scale. Zeolite Y-0.20-S showed the greatest stability during the deactivation/regeneration cycles, with high conversion rates and high selectivity for the production of high quality gasoline. The values obtained correspond to the typical percentages found in the refinery, with conversions greater than 70 wt% and gasoline selectivities around 40 wt%. Zeolites with a higher concentration of mesopores exhibited the greatest selectivity for coke, while also exhibiting improved resistance to coke-induced deactivation during the deactivation/regeneration cycles. In these hierarchical zeolites, we observed a predominance of aromatic coke, which has a higher degree

Table 9
Total acidity (μmol Py/g) and acid site distributions ($\mu mol_{Py}/g$) in fresh, coked, and regenerated zeolites after the last deactivation cycle. (Conversion approximately 60 % wt.).

	Y-0.00-S			Y-0.10-S			Y-0.20-S			Y-0.30-S		
	fresh	coked	regen	fresh	coked	regen	fresh	coked	regen	fresh	coked	regen
Total Acidity (μmol Py/g)	180	103	122	194	112	135	209	118	197	184	61	163
Type of sites (%)												
B	60	25	51	55	22	48	56	20	43	63	35	53
L	40	75	49	45	78	52	44	80	57	37	65	47
Acid strength (%)												
weak	65	76	69	72	77	69	70	69	59	58	75	52
strong	35	24	31	28	23	31	30	31	41	42	25	48

of condensation and is primarily composed of 3- and 4-membered rings. Acid and textural properties were affected by coke deposition after the cracking reactions. Reductions in acidity, specific surface area, pore volume, and average mesopore diameter were observed. Additionally, a notable trend was observed in the selectivity of coke towards Brønsted acid sites. Overall, the zeolite regeneration process successfully restored a significant portion of their acid and textural properties, showcasing the efficacy of this treatment in removing the majority of the coke deposits. It was possible to observe that the zeolites with the highest degree of mesoporosity (Y-0.20 and Y-0.30-S) showed greater resistance to deactivation, retaining most of their textural and acid properties, the main ones responsible for their activity and selectivity. In general terms, it is important to study the impact of deactivation on zeolite properties, as the focus is not only on materials that yield high conversions but also on those that remain stable through multiple deactivation/regeneration cycles and demonstrate selectivity towards the desired products. In this regard, Y-0.20-S zeolites show significant potential for utilization in preparing a commercial catalyst targeted toward gasoline production, thereby promoting the energy balance of the FCC process.

Data availability statement

Data will be made available on request.

CRediT authorship contribution statement

Jayson Fals: Writing – review & editing, Writing – original draft, Methodology, Investigation, Conceptualization. **Maria L. Ospina-Castro:** Writing – review & editing, Writing – original draft, Methodology, Investigation. **Andrea Ramos-Hernández:** Writing – review & editing, Writing – original draft, Methodology, Investigation. **Leonardo Pacheco-Londoño:** Writing – review & editing, Writing – original draft, Investigation. **Sonia Bocanegra:** Writing – review & editing, Writing – original draft, Validation, Investigation.

Declaration of competing interest

The authors declare that they have no known competing financial interests or personal relationships that could have appeared to influence the work reported in this paper.

Acknowledgements

Authors kindly acknowledge their respective Universities for providing kind support.

References

[1] J. Zhou, J. Zhao, J. Zhang, T. Zhang, M. Ye, Z. Liu, Regeneration of catalysts deactivated by coke deposition: a review, Chin. J. Catal. 41 (2020) 1048–1061, https://doi.org/10.1016/s1872-2067(20)63552-5.
[2] P. Chaiwang, H. Chitcharoenyoo, P. Piumsomboon, B. Chalermsinsu, Effect of a pulsating flow on hydrodynamics and fluid catalytic cracking chemical reaction in a circulating fluidized bed riser, Particuology 67 (2022) 47–56, https://doi.org/10.1016/j.partic.2021.10.002.
[3] Y. Zhang, X. Lu, R. Owen, G. Manos, R. Xu, F. Wang, W. Maskell, P. Shearing, D. Brett, Fine structural changes of fluid catalytic catalysts and characterization of coke formed resulting from heavy oil devolatilization, Appl. Catal. B Environ. 263 (2020) 118329, https://doi.org/10.1016/j.apcatb.2019.118329.
[4] J. Garcia, J. Fals, L. Dietta, U. Sedran, VGO from shale oil. FCC processability and co-processing with conventional VGO, Fuel 328 (2022) 125327, https://doi.org/10.1016/j.fuel.2022.125327.
[5] K. Peters, X. Xia, A. Pomerantz, O. Mullins, Geochemistry applied to evaluation of unconventional resources, in: Y. Zee Ma, S. Holditch (Eds.), Unconventional Oil and Gas Resources Handbook: Evaluation and Development, 2016, pp. 71–126. Amsterdam: Gulf Professional.
[6] Z. Caineng, Z. Rukai, T. Shizhen, H. Lianhua, X. Yuan, G. Zhang, Unconventional Petroleum Geology, second ed., Elsevier, Amsterdam, 2017, p. 300. ISBN 9780128122341.
[7] M. Shah, R. Utikar, V. Pareek, G. Evans, J. Joshi, Computational fluid dynamic modelling of FCC riser: a review, Chem. Eng. Res. Des. 111 (2016) 403–448, https://doi.org/10.1016/j.cherd.2016.04.017.
[8] Q. Almas, M. Naeem, M. Baldanza, J. Solomon, J. Kenvin, C. Müller, V. Teixeira da Silva, C. Jones, C. Sievers, Transformations of FCC catalysts and carbonaceous deposits during repeated reaction-regeneration cycles, Catal. Sci. Technol. 9 (2019) 6977–6992, https://doi.org/10.1039/c9cy01680e.
[9] S. Mahamulkar, K. Yin, P. Agrawal, R. Davis, C. Jones, A. Malek, H. Shibata, Formation and oxidation/gasification of carbonaceous deposits: a Review, Ind. Eng. Chem. Res. 55 (2016) 9760–9818, https://doi.org/10.1021/acs.iecr.6b02220.
[10] J. Garcia, M. Falco, U. Sedran, Intracrystalline mesoporosity over Y zeolites. Processing of VGO and resid-VGO mixtures in FCC, Catal. Today 296 (2017) 247–253, https://doi.org/10.1016/j.cattod.2017.04.010.
[11] J. Fals, J.R. García, M. Falco, U. Sedran, Performance of equilibrium FCC catalysts in the conversion of the SARA fractions in VGO, Energy Fuels 34 (2020) 16512–16521, https://doi.org/10.1021/acs.energyfuels.0c02804.
[12] S. Batool, V. Sushkevich, J. Bokhoven, Factors affecting the generation and catalytic activity of extra-framework aluminum Lewis acid sites in aluminum-exchanged zeolites, ACS Catal. 14 (2024) 678–690, https://doi.org/10.1021/acscatal.3c04195.
[13] A. Corma, E. Corresa, Y. Mathieu, L. Sauvanaud, S. Al-Bogami, M.S. Al-Ghrami, A. Bourane, Crude oil to chemicals: light olefins from crude oil, Catal. Sci. Technol. 7 (2017) 12–46, https://doi.org/10.1039/C6CY01886F.
[14] N. Zimmermann, M. Haranczyk, History and utility of zeolite framework-type discovery from a data-science perspective, Cryst. Growth Des. 16 (2016) 3043–3048, https://doi.org/10.1021/acs.cgd.6b00272.
[15] J. Fals, J. Garcia, M. Falco, U. Sedran, Coke from SARA fractions in VGO. Impact on Y zeolite acidity and physical properties, Fuel 225 (2018) 26–34, https://doi.org/10.1016/j.fuel.2018.02.180.
[16] J. Groen, W. Zhu, S. Brouwer, S. Huynink, F. Kapteijn, J. Moulijn, J. PérezRamírez, Direct demonstration of enhanced diffusion in mesoporous ZSM-5 zeolite obtained via controlled desilication, J. Am. Chem. Soc. 129 (2007) 355–360, https://doi.org/10.1021/ja065737o.
[17] H.S. Cerqueira, G. Caeiro, L. Costa, F. Ramôa Ribeiro, Deactivation of FCC catalysts, J Mol Catal A: Chem 292 (2008) 1–13, https://doi.org/10.1016/j.molcata.2008.06.014.

[18] S. Haitao, D. Zhijian, Z. Yuxia, T. Huiping, Effect of coke deposition on the remaining activity of FCC catalysts during gas oil and residue cracking, Catal. Commun. 16 (2011) 70–74, https://doi.org/10.1016/j.catcom.2011.09.001.
[19] A. Amaya, C. Gonzales, F. Martinez, The behavior of the surface Si/(Si+Al) ratio in the FCC catalyst deactivation, J. Electron. Spectrosc. Relat. Phenom. 239 (2020) 146932, https://doi.org/10.1016/j.elspec.2019.146932.
[20] R. Sadeghbeigi, Fluid Catalytic Cracking Handbook, fourth ed., Butterworth-Heinemann, Oxford, 2020.
[21] F. Passamonti, G. De la Puente, U. Sedran, Comparison between MAT flow fixed bed and batch fluidized bed reactors in the evaluation of FCC catalysts. Conversion and yields of the main hydrocarbon groups, Energy Fuels 23 (2009) 1358–1363, https://doi.org/10.1021/ef8008103.
[22] S. Al-Khattaf, M. Saeed, A. Aitani, M. Klein, Catalytic cracking of light crude oil to light olefins and naphtha over E-cat and MFI: MAT versus ACE and effect of high reaction temperature, Energy Fuels 32 (2018) 6189–6199, https://doi.org/10.1021/acs.energyfuels.8b00691.
[23] D. Stratiev, I. Shishkova, I. Petrov, D. Yordanov, V. Toteva, Investigation of fuid catalytic cracking catalyst performance in a laboratory ACE FCC unit during processing gas oils containing H-Oil gas oils with a variable quality and a variable quantity, Pet Coal 62 (2020) 1485–1496.
[24] A. Ibarra, A. Veloso, J. Bilbao, J. Arandes, P. Castaño, Dual coke deactivation pathways during the catalytic cracking of raw bio-oil and vacuum gasoil in FCC conditions, Appl. Catal., B 182 (2016) 336–346, https://doi.org/10.1016/j.apcatb.2015.09.044.
[25] J. Fals, C. Toloza, E. Puelo-Polo, E. Marquez, F. Méndez, A comprehensive study of product distributions and coke deposition during catalytic cracking of vacuum gas oil over hierarchical zeolites, Heliyon 9 (2023) 15408, https://doi.org/10.1016/j.heliyon.2023.e15408.
[26] J. Fals, Garcia-Valencia, E. Puello-Polo, F. Tuler, E. Marquéz, Hierarchical Y zeolite-based catalysts for VGO cracking: impact of carbonaceous species on catalyst acidity and specific surface area, Molecules 29 (2024) 3085, https://doi.org/10.3390/molecules29133085.
[27] ASTM, Standard Test Method for API Gravity of Crude Petroleum and Petroleum Products (Hydrometer Method), ASTM international, 2019, p. D287, 12b.
[28] ASTM, Standard Test Method for Determination of Carbon Residue (Micro Method), ASTM international, 2020, p. D4530, 15.
[29] ASTM, Standard Test Method for Characteristic Groups in Rubber Extender and Processing Oils and Other Petroleum-Derived Oils by the Clay-Gel Absorption Chromatographic Method, ASTM international, 2016, pp. D2007–D2011.
[30] ASTM, Standard Test Method for Boiling Range Distribution of Petroleum Fractions by Gas Chromatography, ASTM international, 2023, p. D2887, 23.
[31] C. Emeis, C. Determination of integrated molar extinction coefficients for infrared absorption bands of pyridine adsorbed on 859 solid acid catalysts, J. Catal. 141 (1993) 347–354, https://doi.org/10.1006/jcat.1993.1145, 15408.
[32] V. Zholobenko, C. Freitas, M. Jendrlin, P. Bazin, A. Travert, F. Thibault-Starzyk, Probing the acid sites of zeolites with pyridine: quantitative AGIR measurements of the molar absorption coefficients, J. Catal. 385 (2020) 52–60, https://doi.org/10.1016/j.jcat.2020.03.003.
[33] P. Magnoux, P. Roger, C. Canaff, V. Fouche, N.S. Gnep, M. Guisnet, New technique for the characterization of carbonaceous compounds responsible for zeolite deactivation, Stud. Surf. Sci. Catal. 34 (1987) 317–330, https://doi.org/10.1016/S0167-2991(09)60370-0.
[34] B. Behera, S. Ray, I. Singh, Structural characterization of FCC feeds from Indian refineries by NMR spectroscopy, Fuel 87 (2008) 2322–2333, https://doi.org/10.1016/j.fuel.2008.01.001.
[35] P. Nilsson, J. Otterstedt, Effect of composition of the feedstock on the catalytic cracking of heavy vacuum gas oil, Appl. Catal. 33 (1987) 145–156.
[36] J. Ancheyta, F. Lopez, E. Aguilar, Correlations for predicting the effect of feedstock properties on catalytic cracking kinetic parameters, Ind. Eng. Chem. Res. 37 (1998) 4637–4640.
[37] C. Xu, J. Gao, S. Zhao, S. Lin, Correlation between feedstock SARA components and FCC product yields, Fuel 84 (2005) 669–674, https://doi.org/10.1016/j.fuel.2004.08.009.
[38] N. Ramirez, D. Pérez, C. Trujillo, Zeolites mesoporosity evaluation using the cracking of 1,3,5-triisopropylbenzene; a critical assessment, Microporous Mesoporous Mater. 360 (2023) 112700, https://doi.org/10.1016/j.micromeso.2023.112700.
[39] A. Talebian, S. Tarighi, Synthesis of hierarchical Y and ZSM-5 zeolites using post-treatment approach to maximize catalytic cracking performance, J. Ind. Eng. Chem. 88 (2020) 167–177, https://doi.org/10.1016/j.jiec.2020.04.009.
[40] V. Hoan, U. Armbruster, A. Martin, Micro/mesoporous zeolitic composites: recent developments in synthesis and catalytic applications, Catalysts 6 (2016) 183/1–183/23. https://doi-org.ezproxy.unal.edu.co/10.3390/catal6120183.
[41] A. Ishihara, Preparation and reactivity of hierarchical catalysts in catalytic cracking, Fuel Process. Technol. 194 (2019) 106116, https://doi.org/10.1016/j.fuproc.2019.05.039.
[42] F. Meirer, S. Kalirai, D. Morris, S. Soparawalla, Y. Liu, G. Mesu, J. Andrews, B. Weckhuysen, Life and death of a single catalytic cracking particle, Sci. Adv. 3 (2015) 400199, https://doi.org/10.1126/sciadv.1400199.
[43] E. Derouane, J. Védrine, R. Pinto, P. Borges, L. Costa, M. Lemos, F. Lemos, F. Ribeiro, The acidity of zeolites: concepts, measurements and relation to catalysis. A review on experimental and theoretical methods for the study of zeolite acidity, Catal. Rev. Sci. Eng. 55 (2013) 454–515, https://doi.org/10.1080/01614940.2013.822266.
[44] T. de Oliveira, 4° Encuentro Sudamericano de Craqueo Catalítico, 2000, p. 101. Manaus, Brasil, Anales.
[45] G. Jimenez, R. Aguilar, R. Maya, The fluidized-bed catalytic cracking unit building its future environment, Fuel 90 (2011) 3531–3541, https://doi.org/10.1016/j.fuel.2011.03.045.
[46] A. Oloruntoba, Y. Zhang, C. Samuel, State-of-the-Art review of fluid catalytic cracking (FCC) catalyst regeneration intensification technologies, Energies 15 (2022) 2061, https://doi.org/10.3390/en15062061.
[47] J. Biswas, I. Maxwell, Recent process- and catalyst-related developments in fluid catalytic cracking, Appl. Catal. 63 (1990) 197, https://doi.org/10.1016/S0166-9834(00)81716-9.
[48] H. Yamazaki, H. Hasegawa, C. Tanaka, Y. Takamiya, T. Mitsui, T. Mizuno, Al ion-exchanged USY in FCC catalyst for high LPG yield, Catal. Commun. 159 (2021) 106354, https://doi.org/10.1016/j.catcom.2021.106354.
[49] D. Stratiev, S. Nenov, I. Shishkova, B. Georgiev, G. Argirov, R. Dinkov, D. Yordanov, V. Atanassova, P. Vassilev, K. Atanassov, Commercial investigation of the ebullated-bed vacuum residue hydrocracking in the conversion range of 55–93, ACS Omega 5 (2020) 33290–33304, https://doi.org/10.1021/acsomega.0c05073.
[50] A. Lappas, D. Patiaka, B. Dimitriadis, I. Vasalos, Separation characterization and catalytic cracking kinetics of aromatic fractions obtained from FCC feedstocks, Appl Catal A 152 (1997) 7–26, https://doi.org/10.1016/S0926-860X(96)00337-7.
[51] J. Garcia, M. Johnson, J. Valla, K. Li, J.Y. Ying, Mesostructured zeolite Y - high hydrothermal stability and superior FCC catalytic performance, Catal. Sci. Technol. 9 (2012) 87–94, https://doi.org/10.1039/c2cy00309k.
[52] C. Mota, R. Rawet, Mechanism of aromatic hydrocarbon formation in FCC naphtha, Ind. Eng. Chem. Res. 34 (1995) 4326–4332, https://doi.org/10.1021/ie00039a024.
[53] J. Garcia, M. Bertero, M. Falco, U. Sedran, Catalytic cracking of bio-oils improved by the formation of mesopores by means of Y zeolite desilication, Appl Catal A 503 (2015) 1–8, https://doi.org/10.1016/j.apcata.2014.11.005.
[54] H. Park, H. Heo, J. Jeon, J. Kim, R. Ryoo, K. Jeong, Y. Park, Highly valuable chemicals production from catalytic upgrading of radiata pine sawdust-derived pyrolytic vapors over mesoporous MFI zeolites, Appl Catal B: Env 95 (2010) 365, https://doi.org/10.1016/j.apcatb.2010.01.015.
[55] A. Foster, J. Cheng, Y. Huber, G. Lobo, Optimizing the aromatic yield and distribution from catalytic fast pyrolysis of biomass over ZSM-5, Appl Catal A General 423 (2012) 54–61, https://doi.org/10.1016/j.apcata.2012.02.030.
[56] M. Choi, K. Na, J. Kim, Y. Sakamoto, O. Terasaki, R. Ryoo, Stable single-unit-cell nanosheets of zeolite MFI as active and long-lived catalysts, Nature 461 (2009) 246, https://doi.org/10.1038/nature08288.
[57] H. Mochizuki, T. Yokoi, H. Imai, S. Namba, J.N. Kondo, T. Tatsumi, Effect of desilication of H-ZSM-5 by alkali treatment on catalytic performance in hexane cracking, Appl Catal A 449 (2012) 188–197, https://doi.org/10.1016/j.apcata.2012.10.003.
[58] M. Rodrigues, C. Okolie, C. Sievers, L. Martins, Organosilane-assisted synthesis of hierarchical MCM-22 zeolites for condensation of glycerol into bulky products, Cryst. Growth Des. 19 (2019) 231–241, https://doi.org/10.1021/acs.cgd.8b01310.

[59] L. Silva, J. Stellato, M. Rodrigues, B. Hare, J. Kenvin, A. Bommarius, L. Martins, C. Sievers, Reduced deactivation of mechanochemically delaminated hierarchical zeolite MCM-22 catalysts during 4-propylphenol cracking, J. Catal. 411 (2022) 187–192, https://doi.org/10.1016/j.jcat.2022.05.004.
[60] M. Guisnet, P. Magnoux, Organic chemistry of coke formation, Appl. Catal A 212 (2001) 83–96, https://doi.org/10.1016/S0926-860X(00)00845-0.
[61] I. Hita, H. Mohamed, Y. Attada, N. Zambrano, W. Zhang, A. Ramírez, P. Castaño, Direct analysis at temporal and molecular level of deactivating coke species formed on zeolite catalysts with diverse pore topologies, Catal. Sci. Technol. 13 (2023) 1288–1300, https://doi.org/10.1039/d2cy01850k.
[62] W. Gilbert, E. Morgado, M. de Abreu, G. de la Puente, F. Passamonti, U. Sedran, A novel fluid catalytic cracking approach 749 for producing low aromatic LCO, Fuel Process. Technol. 92 (2011) 750 2235–2240.
[63] P. Jacobs, J. Martens, Chapter 12 introduction to acid catalysis with zeolites in hydrocarbon reactions, Stud. Surf. Sci. Catal. 58 (1991) 445–496.